Journal of the Earth & Space Physics. Vol. 38, No. 3, 2012, P. 1-16

Estimation of the kinematic source parameters and frequency dependent shear wave attenuation coefficient of the 18th June, 2007 Kahak-Qom earthquake in north central Iran

Rahimi, H.[1] and Javan-Doloei, G.[2*]

[1]*Assistant Professor, Earth Physics Department, Institute of Geophysics, University of Tehran, Iran*
[2]*Assistant Professor, International Institute of Earthquake Engineering and Seismology (IIEES), Tehran, Iran*

(Received: 19 May 2010, Accepted: 03 Jul 2012)

Abstract

In this study, analysis is presented in two steps. In the first step, the theoretical S-wave displacement spectra, conditioned by frequency-independent Q, was fitted with the observed displacement spectra. Therefore corner frequency, moment magnitude and frequency-independent Q for each record were estimated simultaneously and the estimate of error is given in the root-mean-square sense over all the frequencies. In the second step, the corrected observed displacement from source effect was fitted with path term of Brune's source model to estimate frequency dependent shear wave Quality factor. For comparison, Frequency dependent shear wave quality factor also is estimated from spectral decay method. The earthquake in Qom, 18 June 2007 (Ml=5.7), was the largest earthquake in the south of Tehran that recorded on strong motion acceleration stations. The data represented more than 40 accelerograms recorded from Kahak-Qom earthquake in the hypocentral distance range from 18 to 170 km. The source term obtained from inversion was analyzed to estimate various source parameters. Thereby, we estimated seismic moment ($1.86*10^{24}$ dyne-cm), corner frequency (0.72 Hz), source radius (2.33 Km), fault slip (38 cm), source duration (1.5 sec), stress drop (12.3 bars) and moment magnitude (5.4), which are found to be consistent with the corresponding values reported in published studies. The path average value of Q is in the range Q=161 to 1652. The anelastic attenuation coefficient for the region as a whole is estimated in step 2 is $Q_s= 47f^{0.71}$ in frequency range of 1 to 32 Hz. The frequency-independence attenuation for the study region shows that, in general, a Q value is significantly similar to the entire frequency range used than those found in other tectonic areas.

Key words: Source parameters, Quality factor, Generalized inversion, Kahak-Qom earthquake

برآورد پارامترهای کینماتیکی چشمه و بستگی بسامدی ضریب تضعیف موج بُرشی زمین‌لرزه ۲۸ خرداد ۱۳۸٦ کهک- قم

حبیب رحیمی[۱] و غلام جوان دولوئی[۲]

[۱] استادیار، گروه فیزیک زمین، مؤسسه ژئوفیزیک دانشگاه تهران، ایران
[۲] استادیار، پژوهشگاه بین‌المللی زلزله‌شناسی و مهندسی زلزله، تهران، ایران

(دریافت: ۸۹/۲/۲۹، پذیرش نهایی: ۹۱/۴/۱۳)

[*]Corresponding author: Tel: 021-22831116 Fax: 021-22299479 E-mail: javandoloei@iiees.ac.ir

چکیده

در این تحقیق تحلیل داده با تاکید بر دو مرحله صورت گرفته است. در مرحله نخست طیف جابه‌جایی موج بُرشی مستقل از بسامد با طیف جابه‌جایی تجربی مطابقت داده شده است. البته برای هر بسامد، انحراف معیار محاسبه و عرضه شده است. در مرحله دوم، طیف جابه‌جایی با لحاظ کردن تصحیح اثر چشمه زمین‌لرزه مطابق مدل براون برای محاسبه وابستگی بسامدی فاکتور کیفیت به‌کار گرفته شده است. برای فراهم شدن زمینه ارزیابی نتایج، فاکتور کیفیت وابسته به بسامد موج بُرشی از روش تضعیف طیفی نیز محاسبه شده است.

طیف جابه‌جایی یک زمین‌لرزه حاوی اطلاعات ارزشمندی از ویژگی‌های چشمه زمین‌لرزه و خصوصیات محیط مسیر انتشار موج لرزه‌ای است. طیف چشمه زمین‌لرزه را می‌توان از طریق مجذور بسامد، ω^2 مطابق مدل براون (۱۹۷۰) برآورد کرد. در این مدل، تضعیف به صورت ω^2 برای بسامدهای بیش از بسامد گوشه رخ می‌دهد. در این راستا طیف جابه‌جایی چشمه از تبدیل فوریه نگاشت رویداد پس از اجرای فرایند تصحیحات اولیه و تضعیف ناکشسانی محاسبه شده است. تضعیف ناکشسانی موج‌های لرزه‌ای از طریق یک کمیت بدون بُعد تحت عنوان فاکتور کیفیت برآورد می‌شود. تاکنون تحقیقات اندکی برای برآورد فاکتور کیفیت براساس تضعیف ناکشسانی موج‌های لرزه‌ای در گستره فلات ایران صورت گرفته است.

در این تحقیق سعی شده است تا با استفاده از مدل‌سازی معکوس تعمیم یافته و روش حداقل مربعات، پارامترهای چشمه زمین‌لرزه و تضعیف ناکشسانی موج بُرشی ناشی از زمین‌لرزه ۲۸ خرداد ۱۳۸۶ تا فاصله ۱۷۰ کیلومتری از کانون آن محاسبه شود. شایان ذکر است زمین‌لرزه ۲۸ خرداد ۱۳۸۶ با بزرگی $M = 5.7$ بزرگ‌ترین زمین‌لرزه جنوب تهران است که به‌صورت رقومی در چندین ایستگاه شتاب‌نگاری وابسته به مرکز تحقیقات ساختمان و مسکن ثبت شده است. بنابراین، بررسی تضعیف ناکشسانی موج بُرشی این زمین‌لرزه به‌خاطر نزدیکی به مراکز پُرجمعیت مانند قم ، تهران و کرج اهمیت زیادی دارد.

در این تحقیق علی‌رغم وجود حدود پنجاه شتاب‌نگاشت سه مولفه‌ای از زمین‌لرزه قم– کهک، برای افزایش دقت محاسبه پارامترها چشمه فاکتور کیفیت، تنها از چهل شتاب‌نگاشت با کیفیت بسیار خوب استفاده شده است. شکل (۱) مقایسه‌ای از سطح نوفه با سیگنال اصلی موج لرزه‌ای را نشان داده است. مولفه‌های افقی هر شتاب‌نگاشت با اِعمال صافی پایین‌گذر ۲۵ هرتز و چرخش آنها حول زاویه پیش سمت به‌منظور بیشینه کردن دامنه موج بُرشی SH برای اجرای فرایند الگوریتم کینوشیتا (۱۹۹۴) آماده‌سازی شده است. پس از تکمیل مراحل پردازش پارامترهای چشمه زمین‌لرزه محاسبه شدند که عبارت‌اند از: (۱) مقدارگشتاور لرزه‌ای $1.86*10^{24}$ dyne-cm ؛ (۲) بسامد گوشه 0.72 Hz؛ (۳) شعاع چشمه 2.33 Km؛ (۴) میزان لغزش گسل 38 cm؛ (۵) میزان دوام چشمه 1.5 sec؛ (۵) اُفت تنش 12.3 bars؛ (۶) بزرگی گشتاوری 5.4. علاوه برآن ضریب تضعیف ناکشسانی موج بُرشی به‌صورت رابطه $Qs= 47f^{0.71}$ برای فاصله ۱۸ تا ۱۷۰ کیلومتری اطراف چشمه زمین‌لرزه حاصل شد که محدوده قم، تهران، کرج و کاشان را پوشش می‌دهد.

واژه‌های کلیدی: پارامترهای چشمه، زمین‌لرزه کهک قم، فاکتور کیفیت، مدل‌سازی معکوس تعمیم یافته

1 Introduction

On 18 June 2007 at 14:29:50 GMT an earthquake of Ml=5.7 vibrated the capital of Iran, Tehran. The epicenter of the event was located at the east western flank of Tehran, around 100 km from the megacity of Tehran and near to Qom city. This earthquake is important not only because it vibrated the capital of Iran, with almost 12 million inhabitants, but also because no big earthquake at a distance of less than 200 km has affected so far Tehran according to instrumental records (Hamzehloo et al. 2007). Tehran, the capital of Iran, is located in a very high seismic zone at the foot of the southern part of the central Alborz Mountains, which is part of the Alpine-Himalayan orogenic belt. The distribution of historical earthquakes (Figure 1) around Tehran shows that the region has experienced eight large destructive earthquakes with magnitude greater than 7 from 4th B.C to 1830 (Ambraseys and Melville, 1982). Figure 2 shows the location of the 18 June 2007 earthquake and used strong motion stations in this study.

A displacement spectrum contains

valuable information regarding the source and medium characteristics. The source spectrum of an earthquake can be approximated by the omega-square model (Brune, 1970), which has ω^2 decay of high frequencies above the corner frequency. The source displacement spectrum can be estimated from a displacement record after correcting with diminution function, which accounts for the geometrical spreading and anelastic attenuation. The anelastic attenuation of seismic waves is characterized by a dimensionless quantity called quality factor Q (Knopoff, 1964). Until today very few studies have been carried out to understand the attenuation characteristics of the Iranian crust. Examples include the work by Nutlii (1980), Mitchell (1995), Rahimi and Hamzehloo (2008) and Rahimi et al. (2010). An analysis scheme for obtaining source parameters and quality factor Q using the generalized inversion and least-square technique has been presented in this paper in two steps. The work presented here is approximately based on the technique of Fletcher (1995) and Joshi (2006a, 2006b) that used inversion methods. In this paper, the Brune's source model (Brune, 1970) is used together with the propagation filter. This study uses the acceleration data of the Kahak-Qom mainshock recorded by Building and Housing Research Center (BHRC) strong ground motion network. The main objectives of this paper are: (i) to compute the source parameters of these earthquakes by using the acceleration data, and (ii) to compute the frequency-dependent shear wave quality factor in the recorded stations.

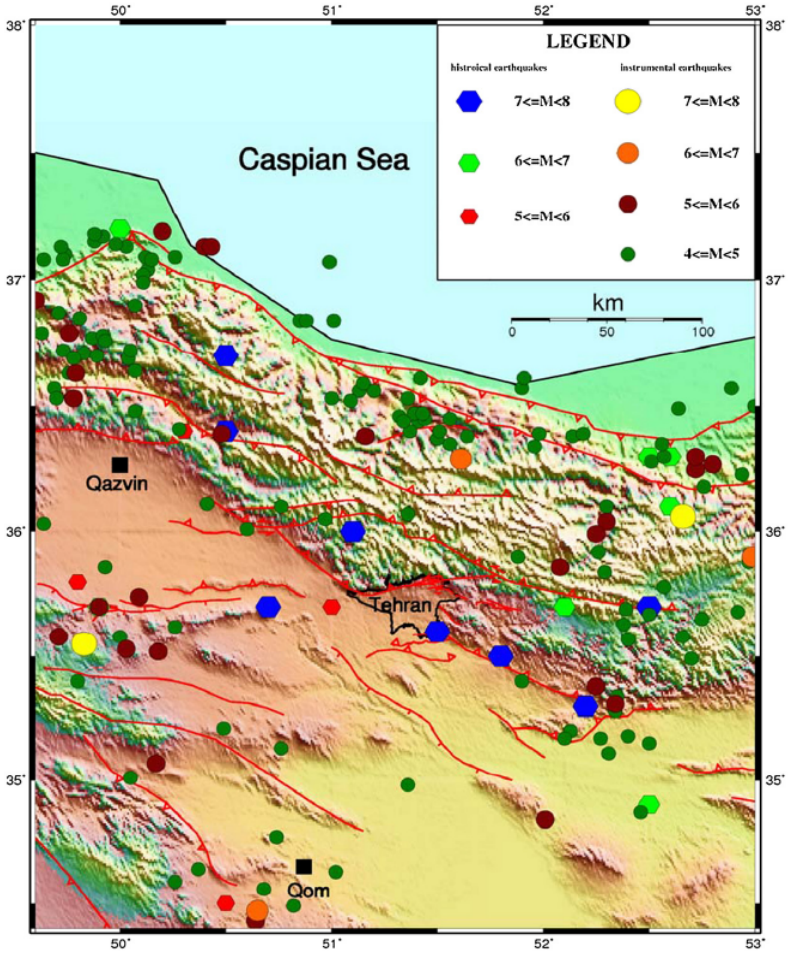

Figure 1. Historical and instrumental earthquakes around Tehran city (Hamzehloo et al., 2007).

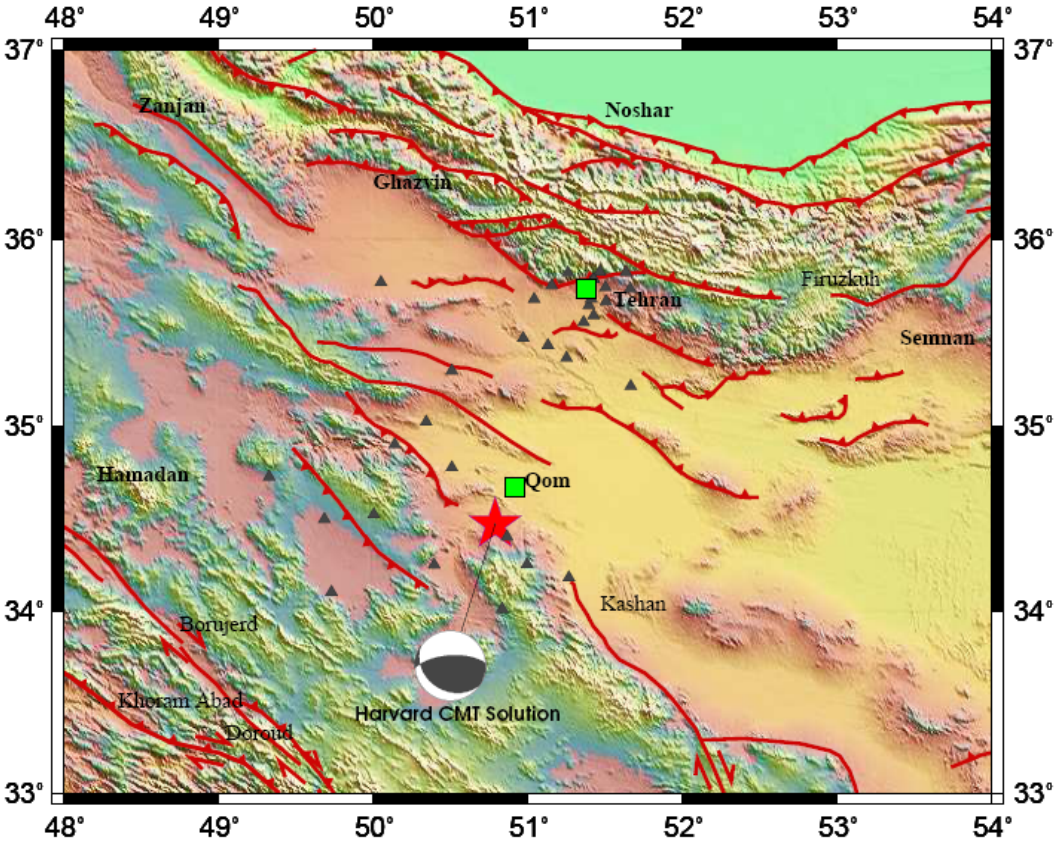

Figure 2. Location map of the Kahak-Qom (2007/06/18) earthquake, strong motion station and faults map.

2 Tectonic setting

Alpine- Himalayan seismic belt is recognized as one of the seismic active areas of the world. Iranian plateau, situated on this belt, has experienced several major and destructive earthquakes in the recent past. Deformation and seismicity in this region is mainly due to the continental shortening between Eurasian and Arabian plates. Iranian plateau is principally divided into five major geological units- based on remarkable tectonic history, magmatic events or sedimentary features (Nabavi, 1976). These units are i) Zagross, ii) Sanandaj-Sirjan, iii) Central Iran , iv) East and South-East zones and v) Alborz, each of which is subdivided into a number of sub-units with specific characteristics. Its deformation is related to the continuous convergent movement between Arabian plate to the southwest and Turan platform to the northeast with the north-northeast drift of Afro-Arabian plate against Eurasia. Iran is one of the seismic active areas of the world and is frequently affected by destructive earthquakes, remaining heavy losses to human life and widespread damage. The Zagros fold-thrust belt as a part of Alpine-Himalayan orogenic belt is one of the youngest and most active contented collision zones on the earth (Synder and Barazangi, 1986) which extends for about 1500 km from Tarus Mountains in southeastern Turkey to fault in the east of strait of Hormoz in Persian Gulf. Highly seismic regions of Alborz-Azarbayjan covered the north and the northwest of Iran, which constitute a part of northern limit of Alpine-Himalayan orogenic belt. Alborz-Azarbayjan major province is a significant belt of seismicity, that covers the northwestern Iran and southern of the Caspian Sea. East-central part of Iran is an intraplate environment between Zagros and kopeh-Dagh fold-thrust border belts. It has

undergone several major organic phases and is characterized by various seismtectonic, metamorphic and magmatic events. Continental collision zone in northeast, Kopeh-Dagh, constituting a part of northern limit of the Alpine-Himalayan mountain belt and its formation is the result of Arabian-Eurasia convergence moments; it is homologous to the Zagros which forms the corresponding southeastern limit of the belt (Tchalenko and Berberian, 1975). Ocean-continental subduction Zone in southeast Iran, Makran, region of southeastern Iran and southern Pakistan is a 1000 km section of the Eurasian-Arabian plate boundary extending from strait of Hormoz in Iran to the mouth of Indus River in Pakistan, where consumption of oceanic crust has occurred continuously since the Early Cretaceous along a north-dipping subduction zone (e.g., Page et al., 1979; Byrne et al., 1992). The covered area in this study is located in the Alborz zone in the North part of Iranian plateau.

3 Data and analysis

The study is based on the accelerograms recorded by the strong motion array maintained by the BHRC. All accelerographs are of Digital SSA-2 type with the threshold of 10 gals at the sampling rate of 200 sample/sec, recording signals from three-component. This configuration yields a flat acceleration response between the frequencies of 0.01 to 50. This earthquake was recorded more than 50 strong motion stations but we used 40 accelerograms that have relatively strong signal to-noise ratios (S/N) of these records enabled a relatively accurate determination of the source parameter and Q factor. As an example of signal and noise level in our records, we illustrated spectral amplitude of shear and noise wave window in Figure 3. To analyze the acceleration records as a fist step, all the recorded waveforms was corrected for drift and baseline by following the algorithm developed by Boore and Bommer (2005). In second step, two horizontal components of acceleration were low-pass filtered, with cutoff frequency at 25 Hz, and then vectorized. The resulting component, a (t), is transverse to the direction of propagation of the earthquake waves and a time window containing the direct SH wave, was selected from the accelerograms by using Kinoshita algorithm (1994). The displacement amplitude spectrum of each acceleration record, at each recording station, was computed by applying Fast Fourier Transform (FFT) to the corresponding time window, and the output of the Fourier transform was post-multiplied by ω^2 to obtain displacement spectrum. Site conditions of most of BHRC stations are unknown and since the SH waves are minimally affected by the crustal heterogeneities (Haskell, 1960; Kumar et. al, 2005), as well as the correction for mode conversion at the surface are not needed, the scattering effects as well as the site amplification effects, which usually are present in limited frequency range are neglected.

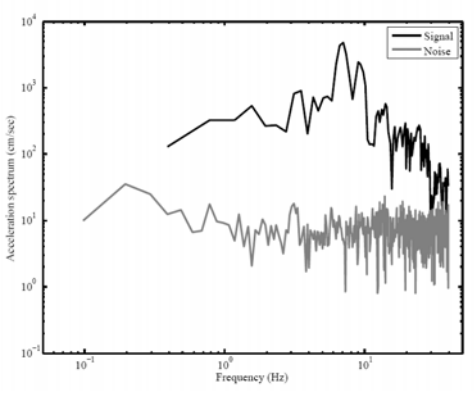

Figure 3. An example of spectral amplitude of shear wave window and noise window for accellerogram recorded in Tehran60 station.

4 Methodology

In this study, analysis is presented in two steps. In the first step, the theoretical S-wave displacement spectra, conditioned by frequency-independent Q, was fitted with the observed displacement spectra via inversion methods. In the second step, the corrected observed displacement from source effect was fitted with path term of Brune's source model to estimate frequency dependent shear wave Quality factor and for comparison, frequency dependence shear wave quality factor also is estimated from spectral decay method.

Step I –Inversion procedure

In this step, we obtained M_0, corner frequency and frequency-independent Q from generalized inversion method for each accelerogram, recorded from Kahak-Qom earthquake. The displacement spectrum of shear waves at distance R due to an earthquake of seismic moment M_0 can be described by (e.g., Boore and Atkinson, 1987; Joshi 2006a, 2006b)

$$D(f) = \frac{C M_0 S(f) e^{-\pi t^* f} R_s(f)}{R} \quad (1)$$

In this expression, C is constant and it is given as (Boore, 1983)

$$C = \frac{R_{\theta\phi} Fs PRTITN}{4\pi\rho\beta^3} \quad (2)$$

where $R_{\theta\varphi}$ is the radiation pattern; F_S is the amplification due to the free surface; *PRTITN* is the reduction factor that accounts for partitioning of energy into two horizontal components; and ρ and β are density, and the shear wave velocity, respectively. $R_s(f)$ is denotes the site amplification factor and the S(f) defines the source spectrum of the earthquake under consideration. In this study, we follow the displacement source spectrum defined by Brune (1970) and therefore consider,

$$S(f) = \frac{1}{1+(f/f_c)^2} \quad (3)$$

Where f_c is the corner frequency, and $f_c = 2.34\beta/2\pi r_0$ with r_0 denoting the radius of the equivalent earthquake source. The exponential term in Equation (1) explains the decay of displacement spectrum with distance due to the anelastic attenuation and scattering. The parameter $t^* = R/Q\beta$ is defined as attenuation time. Equation (1) is linearized by taking natural logarithm:

$$\begin{aligned} &Ln\, D(f) \\ &= Ln\, C + Ln M_0 + Ln\, S(f) \\ &-\pi t^* f - Ln\, R + Ln\, R_s(f) \end{aligned} \quad (4)$$

where t^* and M_0 are unknown parameters. For a known value of f_c, the two unknowns, Q and M_0, can be obtained from inversion by minimizing in the least-square sense, whereas the value of f_c is chosen in an iterative manner. The least square inversion minimizes:

$$\chi^2 = \sum [D_s(f) - S(f)]^2 \quad (5)$$

where $S(f)$ is the source displacement spectrum as proposed by Brune (1970). For the purpose of analysis, Equation (4) is rearranged in the following form:

$$\begin{aligned} &Ln\, M_0 - \pi t^* f \\ &= Ln\, D(f) - Ln\, C \\ &-Ln\, S(f) + Ln\, R - Ln\, R_s(f) \end{aligned} \quad (6)$$

This leads to the following set of Equations for frequencies f_i , i=1,2,3…n where *n is* the total number of displacement spectrum:

$$Ln\, M_0 - \pi\, f_i t^* = K(f_i) \quad (9)$$

With

$$\begin{aligned} &K(f_i) \\ &= Ln\, D(f_i) - Ln\, C - Ln\, S(f_i) + Ln\, R \end{aligned} \quad (10)$$

In matrix form Equation (9) can be written as

$$\begin{bmatrix} 1 & -\pi f_1 \\ 1 & -\pi f_2 \\ \vdots & \vdots \\ 1 & -\pi f_n \end{bmatrix} \begin{bmatrix} Ln\, M_0 \\ t^* \end{bmatrix} = \begin{bmatrix} K(f_1) \\ K(f_2) \\ K(f_3) \\ \vdots \\ K(f_n) \end{bmatrix} \quad (11)$$

The above expression provides a basic statement of the following problem in which the model parameters and the data are in some way related to each other (Menke, 1984):

$$Gm = d \quad (12)$$

Here, *G* represents the rectangular matrix, *m* the model matrix, and *d* the data matrix. Inversion of *G* gives the following model matrix:

$$m = (G^T G)^{-1} G^T d \quad (13)$$

This inversion is prone to problems if G^TG is close to being singular, and for such a case, singular value decomposition (SVD) is used to solve for m (Press et al., 1992). Our formulation of SVD follows Lancose (1961). In this formulation the G matrix is decomposed into U_p, V_p and A_p matrices as (Fletcher, 1995; Joshi, 2006a, 2006b):

$$G^{-1} = V_p A_p U_p^T \quad (14)$$

Where U_p, V_p and A_p have nonzero eigenvectors and eigenvalues.

Step II –Least square and spectral decay methods for frequency dependent Q

1. Least square method for frequency dependent Q

In this step, the corrected observed displacement from source effect was fitted with path term to estimate frequency-dependent shear wave Quality factor. The determined corner frequency and M_0 for each accelerogram in the first step is used to correct its displacement spectrum by dividing source terms. Therefore the frequency-dependent Q has obtained from:

$$Q_s(f) = \frac{-\pi f R}{\beta\{LnD(f) - LnC - Ln\,S(f) - Ln\,M_0 + Ln\,R\}} \quad (15)$$

Where $Q_s(f) = Q_0 f^{\alpha}$ for linearize this Equation, we tacked natural logarithm in each side of Equation (15).

$$Ln\,Q_0 + \alpha Ln\,f = Ln\left\langle \frac{-\pi f R}{\beta\{Ln\,D(f) - LnC - Ln\,S(f) - Ln\,M_0 + Ln\,R\}} \right\rangle \quad (16)$$

From Equation (16) and least square technique Q_0 and α is determined.

2. Spectral decay method

In this method, observed spectral amplitudes at hypocenteral distance, R, from the source are described as:

$$U_i(f,R) = S_i(f) \times A(f,R) \quad (16)$$

where, $U_i(f, R)$ are the observed spectral amplitude for a fixed frequency (f) at hypocenteral distance R from the event i, A(f, R) is the attenuation function that describes the decay trend of the observation toward distance and S(f) is a scaler which depends on the earthquake size. A homogeneous attenuation model is adopted to parameterize A(f, R) as:

$$A(f,R) = R^{-n} e^{-\frac{\pi f t}{Q\beta}} \quad (17)$$

where, f is the frequency, t is the travel time, and β is the velocity of S waves. The geometrical spreading function is represented as R^{-n}. Substituting Equation (17) for Equation (16) yields to:

$$\log U_i(f,R) + n\log R = \log S_i(f) - \pi \log(e)\frac{f}{\beta Q_\beta} R \quad (18)$$

The attenuation functions are obtained by fitting the spectral amplitude decay of the records in the frequency band of 1 to 32 Hz. A decay of 1/R (n=1), implying spherical geometry (R ≤ 100km) and ($1/R^{0.5}$) n=0.5 for R > 100 km, is assumed. Regarding Equation (18), the slope (b) of a linear least square fit of $\{\log U_i(f,R) + n\log R\}$ versus R, corresponds to $-\pi \log(e)\frac{f}{\beta Q_\beta}$ after correcting the observed spectral amplitudes for the effects of geometrical spreading. Thus, to calculate Q_β values, for each designed center

frequency, $Q_\beta = -\frac{\pi \log(e) f}{b\beta}$ is used.

5 Discussion and results

In this study, analysis is presented in two steps and in the first step source parameters and path average independent quality factor has been estimated and in the step 2 frequency dependent quality factor is calculated. Now we discuss on two important steps, separately.

1. First step

In the first step, the theoretical S-wave displacement spectra, conditioned by frequency-independent Q, was fitted with the observed displacement spectra. In this step corner frequency, moment magnitude and frequency-independent Q for each record were estimated simultaneously. The analysis of the strong motion acceleration data has been performed using the model of Burne (1970). Frequency characteristics of this model depend on the corner frequency. As corner frequency is related to the source size, as based on the comparison of the root-mean-square (RMS) error. In right hand of the Figure 4, as an example of step 1 algorithm and in Tehran60 station, the displacement spectra of recorded waveform and the fitted Burne (1970) source model is shown. In the left hand of this figure, the error value between theoretical and observed models for Mw, fc and path average Q parameters from Equation (5) are shown.

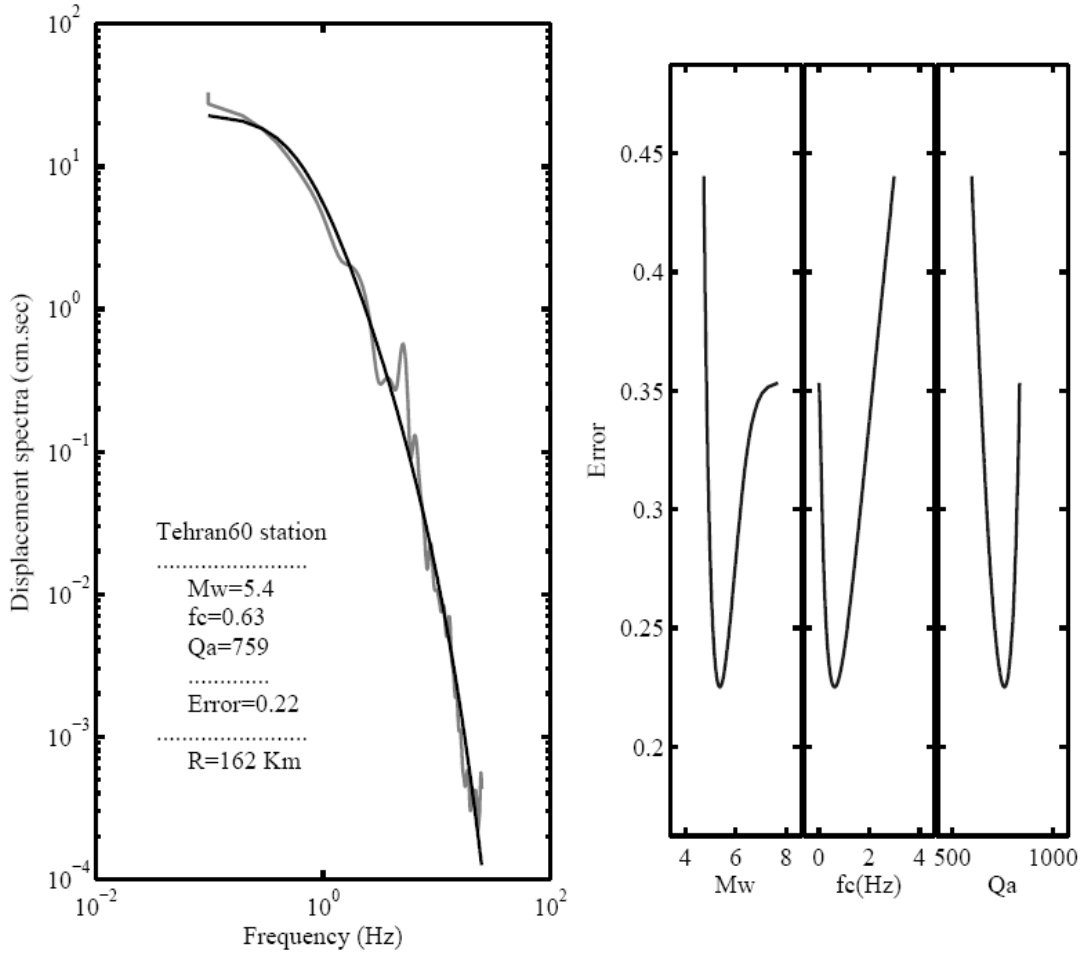

Figure 4. Example of step 1 algorithm in Tehran60 station is shown. The displacement spectra and the fitted Burne (1970) source model in the right hand and in the left hand the error value between theoretical and observed models for Mw, fc and path average Q parameters from Equation (5) are shown.

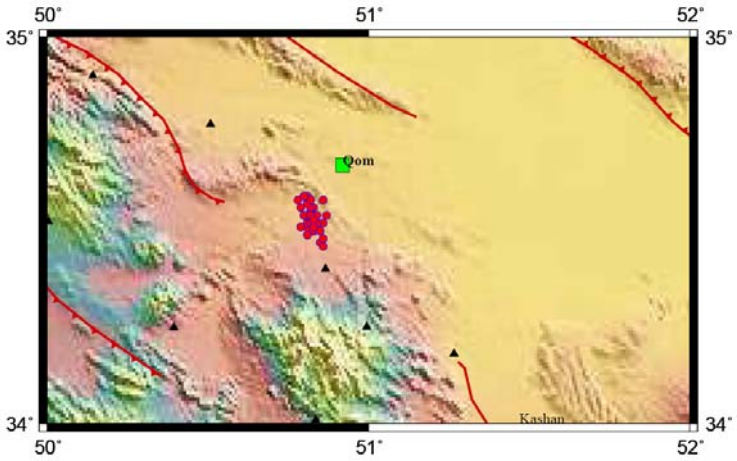

Figure 5. Aftershocks location map of the Kahak-Qom (2007/06/18) earthquake.

The estimated corner frequency values are given in Table 2 for all stations. It has been seen that the mean value of the best estimates of fc for Kahak-Qom earthquake is 0.72 Hz. This best estimation is varied from 0.15 Hz in a Tehran61 station to 1.76 Hz in Mamooniyeh station. Using the estimated corner frequency, the dislocation source radius, r, is obtained from the relation $r_0 = \frac{2.34\beta}{2\pi f_c}$ .Using $\beta = 3.5 km/s$, the source radius is estimated for each station which are given in Table 2. The mean value of source radius for the Kahak-Qom earthquake is calculated as 2.33 Km from this source model. By attention to Wells and Coppersmith, 1994 empirical relationship between rupture length and magnitude, the rupture length is estimated 5 Km that is almost correlated with estimated from Brune's source model. The covering area by the aftershock distribution is projection of the approximately rupture area. The length of aftershock distribution is illustrated in Figure 5 which is about 10 km. Regarding to Wells and Coppersmith (1994) the length of rupture at the surface is equal to 75% of the subsurface rupture length. Thereby, the estimated value for source radius is correlated with rupture area. The average seismic moment for the 40 sites is $M_0 = 1.86 \times 10^{24}\ dyne - cm$. This parameter for each site was calculated from step 1 and is given in Table 2. Using the moment magnitude relation of Hanks and Kanamori (1979),

$$M_w = (2/3)\log M_0 - 10.7 \qquad (19)$$

A moment magnitude values, Mw=5.4, is obtained. In the present work, the stress drop has also been computed using relation from Burne (1971):

$$\Delta\sigma = (7/16)\frac{M_0}{r^3} \qquad (20)$$

These results for each site have been given in Table 2 and the mean value of these parameters in all stations is $\Delta\sigma = 12.3$ bars. The average slip, calculated from $\Delta u = M_0 / \mu\pi r^2$ was estimated as 38 cm using average rigidity, $\mu = 3.5 \times 10^{11}\ dyn/cm^2$ estimated from $\mu = \rho\beta^2$ and this parameter for 40 sites has been given in Table 2. Brune's model assumes a circular dislocation and bidirectional propagation, given source duration as $T_d = r/v_r$, where v_r is the rupture velocity. Assuming that $v_r = 0.85\beta$ gives an estimation of the source duration $T_d = 0.78$ sec. The more realistic estimation is $T_d = 2r/v_r$ that gives 1.56 sec and this is good agreement with the relation $T_d = 1/f_c$ used by Hanks and McGuire (1981)

that gives 1.39 as an estimation for the source duration. The resulting source parameters from local strong motion measurements (M_0=1.86*10^{24} dyne-cm, M_w=5.4) agree remarkably well with the results obtained from Harvard and USGS centers (Table 1). In this step, the average value of shear wave quality factor in frequency range of 1-25 Hz for each acceleration data has been calculated.

The Q obtained as the solution is the value that gives the best overall fit to the data over the spectrum in the frequency band 0.1 to 25 Hz. The estimated Q values were in the range of 161 to 1652, with mean value of 716, and increase with distance as can be seen in Figure 6. This figure shows the variation of path average shear wave quality factor with hypocentral distance that follows Qa = 3.67*R + 197 Equation. Generally, the Q values decreasing with the increase in crust depth is expected. As the rays penetrate to the greater depth in propagating longer distances, the attenuation dependence is expected at the epicentral distances. Thereby, which sites that have a hypocentral distance greater than others, the Q value, obtained at this station is higher than others which may indicate an attenuation of deeper depth rather than shallower one.

Table 1. Parameters of the Kahak-Qom Earthquake of 18th June, 2007.

Origin Time Location Focal depth	**Magnitude Seismic moment**	**Fault-plane solution**	**Reference**
2007 06 18 14:29:54.50 34.470 50.790 18.5	**Mw=5.6 M_0=2.4*10^{24} dyne cm**	**strike=266 dip=41 slip=39**	**CMT (Harvard)**
2007 06 18 14:29:48.29 34.437 50.833 11.0	**Mw=5.5 M_0=1.9*10^{24} dyne cm**	**strike=301 dip=34 slip=62**	**USGS**

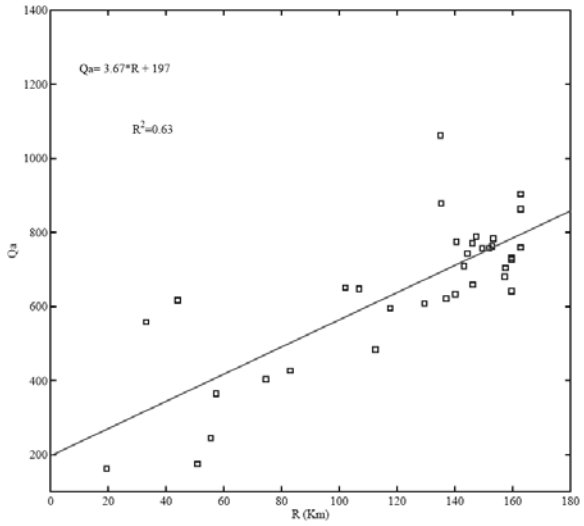

Figure 6. This figure shows the variation of path average shear wave quality factor with epicentral distance.

2. Second step

In this step, the corrected observed displacement from source effect was fitted with path term of Brune's source model to estimate frequency dependent shear wave Quality factor. The determined corner frequency and M_0 for each accelerogram in the first step is used in this step to correct its displacement spectrum from source effect by dividing source terms. For this purpose, 40 accelerograms, recorded at these 40 stations, are used, Table 2. Figure 7 shows estimated Q_s at 5 frequency bands with central frequencies of 1.5, 3, 6, 12 and 24 Hz using Equation (16) and least-square method. The frequency dependent relations of Q_s, estimated in this step is $Q_s= 47f^{0.71}$ in frequency range of 1 to 32 Hz. To check our estimation of frequency-dependence quality factor relation, the second method is used to estimate Qs values in the same previous frequency range. To do this, spectral decay method is used to calculate shear wave quality factor at 5 frequency bands with central frequencies of 1.5, 3, 6, 12 and 25 Hz. For this purpose, 40 accelerograms have been used which were recorded at 40 stations. Figure 8 shows the diagram of Q_s versus central frequencies with linear fitting at frequency band of 1.5, 3, 6, 12 and 24 Hz using spectral decay method. Figure 9 shows frequency dependence of quality factor. The Q_s values, estimated by spectral decay method, vary from 72 at 1.5 Hz to 697 at 24 Hz and the frequency dependent relations of Q_s is $Q_s=54f^{0.79}$ in frequency range of 1 to 32 Hz.

The different Q_s values indicated that the spectral decay method gives higher estimation comparing to method used in step 2. Martinez-Arvalo et al (2003) expressed the Q factor of the medium as the sum of two effects: the near surface attenuation, just below the seismic station and the seismic attenuation of remain path of seismic waves. Based on the analysis of S- wave attenuation, it is observed that method used in step 2 can estimate the seismic attenuation of seismic waves and this way will omit the near surface attenuation. As both wave types have been recorded at the same station, they have the same contribution of the near surface attenuation. Due to above reason, higher values of quality factor obtained from spectral decay method rather than method used in step 2 is reliable.

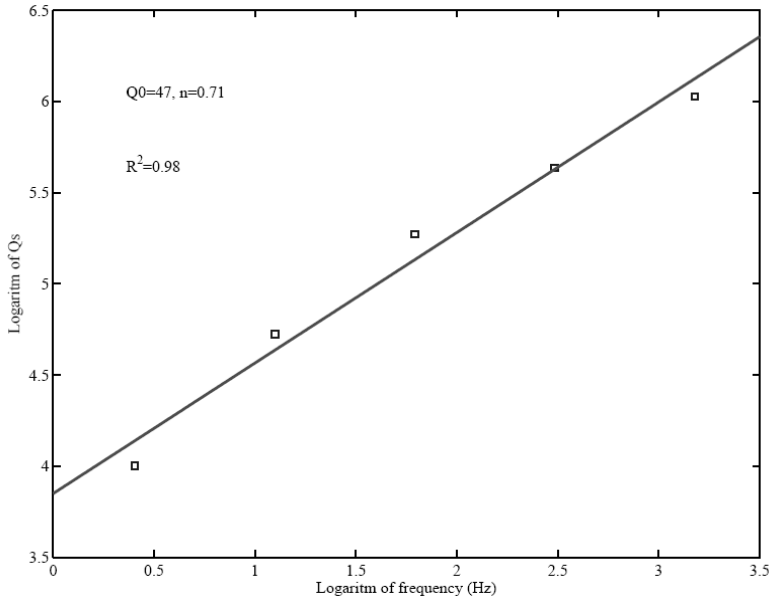

Figure 7. This figure shows estimated Q_s via frequency at 5 frequency bands with central frequencies of 1.5, 3, 6, 12 and 24 Hz using Equation (16) and least-square method.

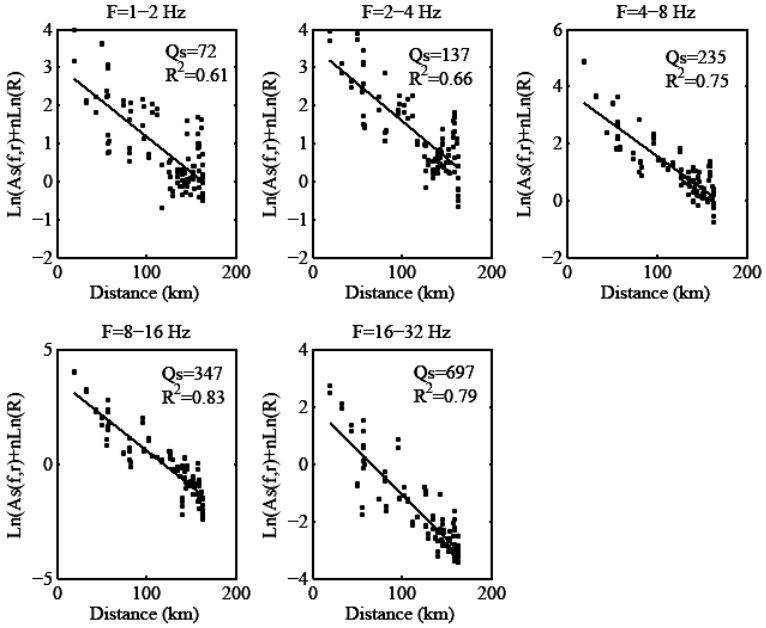

Figure 8. This figure shows the plot of Q_s versus central frequencies with linear regression fit at frequency band of 1.5, 3, 6, 12 and 24 Hz using spectral decay method.

The S-wave attenuation, estimated in this study, is compared with other volcanic, tectonic and seismic active regions of the world (Figure 10). The estimated Q_0 is lower comparing to the Avaj region and is higher than Ardebil region in Iran. This is due to the attenuation of shear waves, which indicates the intrinsic attenuation and it depends on friction, viscosity and thermal relaxation. As the Ardebil region is a volcanic and geothermal area, it has a lower Q_0 values than this study. The frequency dependent shear wave quality factor measurements in other parts of the world show that it follows the trend similar to those of active tectonic regions and close to Guerrero, Mexico as shown in figure 10.

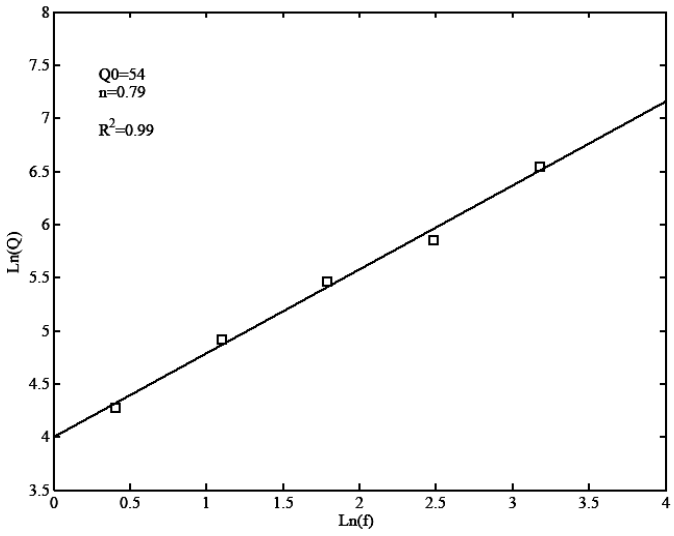

Figure 9. This figure shows frequency dependence of quality factor obtained from spectral decay method.

Table 2. Estimation of Source Parameters, Quality factor and RMS error for each accelorgram in step 1.

Station name	Epicentral Distance (Km)	Fc (Hz)	M0 Dyne-cm	Mw	Path average Q	RMS	Source Radius Km	$\Delta\sigma$ bars	ΔU cm
KAHAK	19.3	0.92	5.35E+23	5.1	162	0.25	1.42	8.23	24.24
Gazoran	50.9	1.25	1.41E+24	5.4	175	0.18	1.04	54.27	117.65
Mashkat	55.5	0.57	1.42E+24	5.4	2451	0.13	2.29	5.18	24.65
Raveh	57.3	0.74	1.11E+24	5.3	364	0.11	1.76	8.91	32.64
Saveh	74.5	0.65	1.23E+24	5.4	403	0.10	2.00	6.65	27.74
Ashtiyan	82.9	0.36	2.86E+24	5.6	427	0.11	3.62	2.63	19.83
Hassan Abad	97.1	0.84	2.54E+24	5.6	429	0.09	1.55	29.70	95.82
Farmahin	112.4	0.63	2.98E+24	5.6	483	0.10	2.06	14.72	63.34
Veshnaveh	33.1	0.35	2.46E+24	5.7	558	0.24	3.72	2.08	16.11
Emam khomaini	117.6	1.12	6.89E+23	5.2	595	0.18	1.16	19.12	46.25
Parand	129.4	1.41	3.99E+23	5.0	608	0.12	0.92	22.12	42.51
Naragh	44.0	0.42	1.49E+24	5.4	616	0.14	3.10	2.18	14.06
Tehran58	136.9	0.94	8.37E+23	5.2	620	0.10	1.38	13.73	39.59
TEHRAN 22	140.1	0.57	1.13E+24	5.3	633	0.24	2.28	4.12	19.61
TEHRAN 36	159.6	1.34	1.21E+24	5.3	641	0.33	0.97	57.46	116.19
Arak	106.8	1.01	7.77E+23	5.2	647	0.11	1.29	15.81	42.43
Javad Abad	102.1	1	8.84E+23	5.3	650	0.20	1.30	17.46	47.31
Komijan	146.1	0.65	1.74E+24	5.5	659	0.13	2.00	9.43	39.33
Lavasan	157.2	0.51	2.85E+24	5.6	680	0.23	2.55	7.46	39.64
Boeen Zahra	157.5	0.92	1.47E+24	5.4	704	0.19	1.41	22.65	66.71
TEHRAN 11	143.1	0.96	7.96E+23	5.2	709	0.14	1.35	13.90	39.24
TEHRAN 32	159.6	0.88	1.66E+24	5.4	727	0.41	1.48	22.38	68.93
TEHRAN 10	159.6	0.42	2.56E+24	5.6	732	0.18	3.10	3.75	24.21
Tehran 54	144.3	0.72	1.01E+24	5.3	742	0.14	1.81	7.44	28.01
TEHRAN 12	151.8	0.42	2.71E+24	5.6	756	0.09	3.10	3.96	25.54
TEHRAN 27	149.5	0.25	7.99E+24	5.9	757	0.14	5.21	2.46	26.73
Tehran60	162.8	0.63	1.26E+24	5.4	759	0.22	2.06	6.29	26.74
TEHRAN 24	152.8	0.74	1.16E+24	5.3	762	0.16	1.76	9.31	34.08
Souleghan	145.9	1.09	7.7E+23	5.2	770	0.21	1.19	19.69	48.96
TEHRAN 9	140.4	0.39	1.4E+24	5.4	774	0.37	3.34	1.63	11.38
TEHRAN 17	153.2	0.51	2.33E+24	5.5	782	0.06	2.55	6.10	32.43
TEHRAN 13	147.3	0.5	2.36E+24	5.5	789	0.21	2.60	5.82	31.58
Tehran61	162.8	0.15	9.55E+24	5.9	863	0.19	8.68	0.63	11.49
TEHRAN 26	135.2	0.48	2.04E+24	5.5	878	0.14	2.71	4.45	25.17
Tehran59	162.8	0.61	9.19E+23	5.3	903	0.13	2.13	4.12	18.30
TEHRAN 29	135.0	0.49	1.47E+24	5.4	1062	0.11	2.66	3.41	18.85
Mamooniyeh	96.2	1.76	3.69E+23	5.0	1152	0.26	0.74	39.78	61.25
Saveh Dam1	80.8	0.25	2.47E+24	5.6	1174	0.16	5.21	0.76	8.27
Shahriyar	127.4	0.64	7.71E+23	5.2	1605	0.15	2.03	3.99	16.90
TEHRAN 1	142.6	0.77	6.98E+23	5.2	1652	0.18	1.69	6.29	22.16

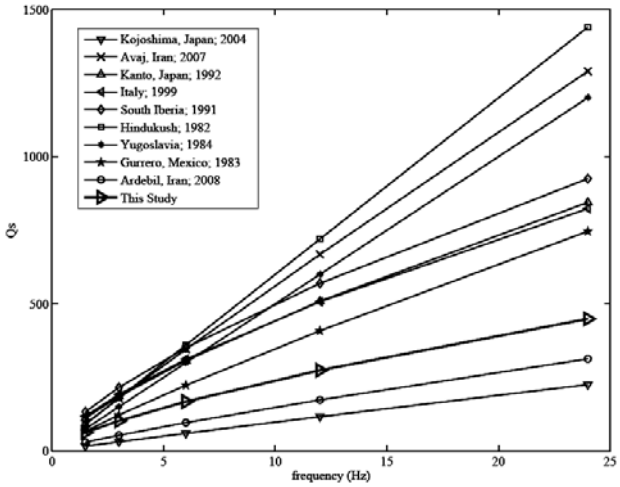

Figure 10. Comparison of shear wave quality factor of Iran region and this study with those reported from other regions of the worlds.

6 Conclusion

In this study, the source parameters and frequency dependent shear wave quality factor has been estimated in two steps. In the first step, the theoretical S-wave displacement spectra, conditioned by frequency-independent Q, was fitted with the observed displacement spectra. In this step corner frequency, moment magnitude and frequency-independent Q for each record were estimated simultaneously. In the second step, the corrected observed displacement from source effect was fitted with path term of Brune's source model to estimate frequency dependent shear wave Quality factor and for comparison, frequency dependence shear wave quality factor also is estimated from spectral decay method.

The following conclusions have emerged from our analysis data.

- We estimated seismic moment ($1.86*10^{24}$ dyne-cm), corner frequency (0.72 Hz), source radius (2.33 Km), fault slip (38 cm), source duration (1.5 sec), stress drop (12.3 bars) and moment magnitude (5.4), which are found to be consistent with the corresponding values reported in published studies.
- The path average value of Q in the frequency range of 1-25 Hz is Q = 161 to 1652 with mean value of 716, and the variation of path average quality factor with epicentral distance follow Qa = 3.67*R + 197 Equation.
- The estimated anelastic attenuation coefficient for the region in step 2 is $Q_s = 47f^{0.71}$ in frequency range of 1 to 32 Hz.
- The Q_s values, estimated by spectral decay method, vary from 72 at 1.5 Hz to 697 at 24 Hz and the frequency dependent relations of Q_s is $Q_s=54f^{0.79}$ in frequency range of 1 to 32 Hz.
- Clear differences as a function of the spectral decay and method used in step 2 are observed; the spectral decay method has supplied significantly higher Q values than the method used in step 2. This discrepancy is interpreted as the methods effects in other similar studies.
- The frequency-independence attenuation for the study region show that, in general, Q values is significantly similar for the entire frequency range used than those found in other tectonic areas.

References

Ambraseys, N. N. and Melville, C. P., 1982, A history of Persian earthquakes, Cambridge University Press, London, 219 pp.

Boore, D. M., 1983, Stochastic simulation of high-frequency ground motion based on

seismological models of the radiated spectra, Bull. Seism. Soc. Am., **73**, 1865-1894.

Boore, D. M. and Atkinson, G. M., 1987, Stochastic prediction of ground motion and spectral response parameters at hard-rock sites in eastern north America, BSSA, **77**(2), 440-467.

Boore, D. M. and Bommer, J. J., 2005, Processing of strong-motion accelerograms: Needs, options and consequences, Soil Dynamics and Earthquake Engineering, **25**, 93-115.

Brune, J. N., 1970, Tectonic stress and the spectra of seismic shear waves from earthquake, J. Geophys. Res., **75**, 5009-4997.

Byrne, D., Sykes, l. and Dav, S. D., 1992, Great thrust earthquake and aseismic slip along the sistan suture zone of eastern Iran, Geophys. J, Int., **136**, 671-694.

Fletcher, J. B, 1995, Source parameters and crustal Q for four earthquakes in South Carolina, Seism, Res. Lett., **66**, 44-58.

Hamzehloo, H., Vaccari, F. and Panza, G. F., 2007, Towards a reliable seismic microzonation in Tehran, Iran, Engineering Geology, **93**, 1-16.

Hanks, T. C. and Kanamori, H., 1979, A moment magnitude scale, J. Geophys. Res., **84**, 2348-2350.

Hanks, T. C. and McGuire, R. K., 1981, the character of high-frequency strong ground motion, Bull. Seism. Soc. Am., **71**, 2071-2095.

Haskell, N. A., 1960, Crustal Reflection of plane SH waves, J. Geophys. Res., **65**, 4147-4150.

Joshi, A, 2006a, Use of acceleration spectra for determining the frequency-dependent attenuation coefficient and source parameters, BSSA, **96**(6), 2165-2180.

Joshi, A., 2006b, Analysis of strong motion data of the Uttarkashi earthquake of 20th October 1991 and the Chamoli earthquake of 28th March 1999 for determining the mid crustal Q value and source parameters, ISET Journal of Earthquake Technology, **468**(43), (1-2), 11-29.

Kinoshita, S., 1994, Frequency-dependent attenuation of shear wave in the crust of the southern kanto area, Bull. Seism. Soc. Am., **59**, 1387-1396.

Knopoff, L., 1964, Q, Reviews of Geophysics, **2**(4), 625-660.

Kumar, D., Sarkar, I., Sriram, V. and Khattri, K. N., 2005, Estimation of the source parameters of the Himalaya earthquake of October 19, 1991, average effective shear wave attenuation parameter and local site effects from accelerograms, Tectonophysics, **407**, 1-24.

Lancose, C., 1961, Linear differential operators, D. Van Nostrand Co. London.

Martinez-Arevalo, C., Bianco, F., Ibanez, J. M. And Del Pezzo, E., 2003, Shallow seismic attenuation and shear wave splitting in the short period range of Deception island volcano (Antarctica), J. Geoth. Res., **128**, 89-113.

Menke, W., 1984, Geophysical data analysis: discrete inverse theory, Academic Press Inc., New York, U.S.A.

Mitchell, B. J., 1995, Anelastic structure and evolution of continental crust and upper mantle from seismic surface wave inversion, Rev. Geophys, **33,** 441-462.

Nabavi M. H., 1976, An introduction to the geology of Iran, Geological Survey of Iran, In Farsi, 110 pp.

Nuttli, O. W., 1980, the excitation and attenuation of seismic crustal phases in Iran, Bulletin of the Seismological Society of America, **70**(2), 469-485.

Page, W, D., Alt, J. N., Gluff, L. S. and Plafker, G., 1979, Evidence for the recurrence of large magnitude earthquake along the Makran coast of Iran and Pakistan, Tectonophusics, **52**, 533-542.

Press, W. H.; Flannery, B. P.; Teukolsky, S. A. and Vetterling, W. T., 1992, Singular value decomposition. §2.6 in numerical recipes in FORTRAN, The Art of Scientific Computing, 2nd ed. Cambridge, England: Cambridge University Press, 51-63.

Rahimi, H. and Hamzehloo, H., 2008, Lapse time and frequency-dependent attenuation of coda waves in the Zagros continental collision zone in the Southwestern Iran, J.

Geophys. Eng.**, 2,** 173-186.

Rahimi, H., Kamalian, H. and Hamzehloo, H., 2010, Estimation attenuation of coda and shear waves in the volcanic area in NW of Iran, Journal of Asian Earth Sciences, under revision.

Snyder, D. B. and Barazangi, M., 1986, Deep crustal structure and flexure of the Arabian plate beneath the Zagros coalitional mountain belt as inferred from gravity observation, Tectonics, **5**, 361-373.

Tchalenko, J. S. and Beberian, M., 1975, Dasht-e-Bayaz fault Iran: earthquake and earlier related structures in bedrock, Geol. Surv. Am. Bull., **86**, 703-709.

Wells, D. L. and Coppersmith, K. L., 1994., New empirical relationships among magnitude, rupture length, rupture width, rupture area, and surface displacement, BSSA, **84**(4), 974-1002.